

Multistep Locked-to-Sliding Transition in a Thin Lubricant Film

O. M. Braun,^{1,2} A. R. Bishop,¹ and J. Röder¹

¹Theoretical Division and Center for Nonlinear Studies, Los Alamos National Laboratory, Los Alamos, New Mexico 87545

²Institute of Physics, National Ukrainian Academy of Sciences, UA-252022 Kiev, Ukraine

(Received 12 November 1998)

Using Langevin simulations, we study dynamical transitions in a model three-layer atomic film confined between two rigid substrates moving with respect to each other. With the increase of a dc force applied to the top substrate, first the middle layer of the lubricant film transitions from locked to sliding states; this regime shows a stick-slip behavior with a relatively high effective friction. Next, the layers closest to the substrates start to slide over the substrates, as well as with respect to the middle layer; the effective friction in this regime may be explained by energy losses due to the excitation of phonons in the lubricant. Finally, at high velocities the lubricant film decouples from the substrates and achieves a “flying” regime characterized by a very low friction coefficient. [S0031-9007(99)08913-9]

PACS numbers: 68.10.-m, 62.20.Qp, 68.60.-p

The problem of friction between two substrates which are in moving contact is very important technologically as well as very rich physically [1]. Following the development of atomic force microscopy, studying tribology has approached the microscopic level. Besides the experimental methods, molecular dynamics (MD) with realistic potentials [2–4] may be useful to provide very detailed information on atomic motions, but such simulations are extremely time consuming. An alternate route is to use microscopic modeling which only incorporates the principal degrees of freedom, such as in simple Frenkel-Kontorova (FK) type models [5–8]. The present work analyzes an intermediate complexity model consisting of three atomic layers. In a previous publication [9] this problem was considered for the commensurate film. Here we study an incommensurate case.

Our three-dimensional system comprises a three atomic-layer film between two solid substrates, the top and bottom. Each substrate has $N_s = 132$ atoms of mass $m_s = 1$ organized into a 12×11 lattice of square symmetry with the lattice constants $a_{sx} = a_{sy} = 3$. The film situated between the substrates consists of $N_a = 240$ atoms of mass $m_a = 1$. In the x and y directions we use periodic boundary conditions. The atoms of the bottom substrate are fixed at their lattice sites \mathbf{r}_n ($1 \leq n \leq N_s$), while the top substrate moves rigidly. The positions of the top substrate atoms are therefore given by $\mathbf{U} + \mathbf{r}_n$, where \mathbf{U} is the vector describing the motion of the top substrate. The atoms of the film have positions denoted by \mathbf{u}_m ($1 \leq m \leq N_a$). Top substrate and film atoms may move in all three dimensions. All atoms interact via the 6–12 Lennard-Jones potential $V^{(x)}(r) = V_x[(r_x/r)^{12} - 2(r_x/r)^6]$. We use different parameters V_x and r_x for the interaction within the film, “ $x = a$,” and the interaction of the film atoms with the substrates, “ $x = 0$.” This simulates a lubricant between two solids.

Although we work with dimensionless quantities, the numerical values of the model parameters have been

chosen such that, if energy were measured in electron volts and distances in angstroms, we would have realistic values for a typical solid. We took $V_0 = 3$ and $r_0 = 3$ for the interaction of atoms of the film with the substrates, giving a typical frequency for the system of $\omega_0 = 6\sqrt{2V_0/m_a r_0^2} = 4.9$ and the corresponding characteristic period is $\tau_0 \equiv 2\pi/\omega_0 = 1.28$. For the interatomic interaction within the film we took $V_a = 1$. Because $V_a \ll V_0$, some atoms of the film will tend to stick to the top and bottom substrates, covering them with monolayers, while the others fill the space between these monolayers. Here we study the “incommensurate” lubricant film with $r_a = 4.14$. In this case the equilibrium configuration of the film corresponds to three layers, each having 80 atoms, organized into a close-packed triangular lattice slightly distorted by the substrate potentials. A typical frequency of vibrations within the layer is $\omega_a = 6\sqrt{2V_a/m_a r_a^2} = 2.05$.

To each atom of the top substrate we apply a dc force \mathbf{F} , consisting of a driving force f along the x axis and a loading force $f_{\text{load}} = -0.1$ along the z direction. The Langevin equations for the system are therefore

$$\begin{aligned}
 N_s \ddot{\mathbf{U}} &= N_s \mathbf{F} - \sum_{m',n} \nabla V^{(0)}(|\mathbf{u}_{m'} - \mathbf{U} - \mathbf{r}_n|), \\
 \ddot{\mathbf{u}}_m + \eta \dot{\mathbf{u}}_m &= \mathbf{F}_m^{\text{rand}} - \sum_{m'} \nabla V^{(a)}(|\mathbf{u}_m - \mathbf{u}_{m'}|) \\
 &\quad - \sum_n \nabla V^{(0)}(|\mathbf{u}_m - \mathbf{U} - \mathbf{r}_n|),
 \end{aligned} \tag{1}$$

where $\mathbf{F}_m^{\text{rand}}$ are the random Langevin forces required to equilibrate the system to the temperature $T = 0.025$, which corresponds to room temperature for energies measured in eV. A uniform external viscous friction, $\eta = 0.1 \omega_0 = 0.49$, models the energy exchange between the layer and the substrates as well as that due to other missing degrees of freedom such as electron-hole excitations. The substrate acts as a thermostat and

feels no external damping. The simulation algorithm is identical to that described in [9] with a force step of 0.001.

The simulation results are summarized in Fig. 1, which shows the velocity of the top substrate and the average film velocity in the x direction as functions of the driving force. Each plotted point is the average over 100 data points recorded at times separated by $\Delta t = \tau_0$. We clearly see that the following regions can be identified.

(I) At low forces, $f \leq f_s = 0.145$, the top substrate is immobile. The value f_s corresponds to the static frictional force. f_s is about an order of magnitude lower than that for the commensurate lubricant film for the same model parameters [9]. When f increases beyond f_s , the top substrate, together with the one atomic layer attached to it, starts to slide over the middle layer which, in turn, slides over the immobile bottom substrate with its one attached layer. Examining atomic trajectories, we have observed that at the transition all atoms in the middle layer start to slide almost simultaneously, i.e., the transition has a more global than local character.

(IIa) For forces $0.146 \leq f \leq 0.485$, the average velocity of the top substrate is $\langle v_s \rangle \approx (1.4-2)f$. In the following we term this state the “running-I” state. As can be seen from Figs. 2b and 2c, here the lubricant film splits into three layers; the bottom and top ones are attached to the corresponding substrates, while the middle layer slides over the bottom layer as well as with respect to the top layer, and moves with an average velocity $\langle v_m \rangle \approx 0.5\langle v_s \rangle$. The structure of the middle layer is reminiscent of a “solid with defects” (i.e., the layer does not have the ideal triangular structure, but certainly does not resemble a liquid), although the atomic trajectories are

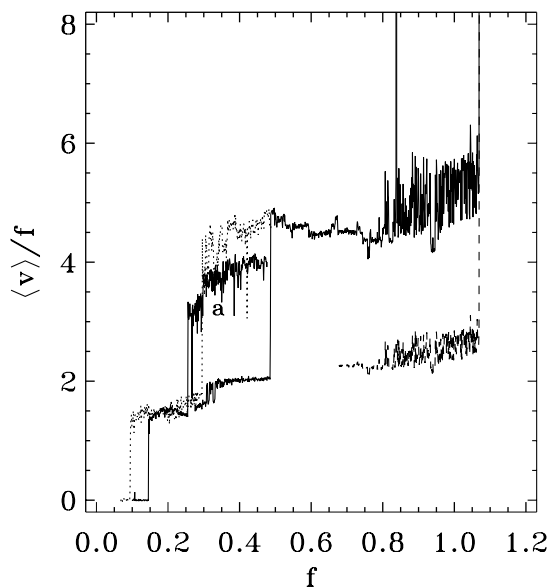


FIG. 1. The ratio $\langle v \rangle / f$ versus f . The solid curve corresponds to the increasing force, and the dotted curve corresponds to the decreasing force. The dashed curve describes the velocity of the film atoms only, averaged over all 240 atoms of the film.

quite irregular. This steady state may be called a “stick-slip motion on an atomic scale,” similar to what has been observed in [8] for simpler models, i.e., the middle layer moves for some relaxation time and then stops (sticking to the top or bottom layers), waiting until the stress again reaches the threshold value. Because the stick-slip transitions occur randomly in time, this regime is characterized by the low-frequency power spectrum $\langle v_m^2 \rangle(\omega) \propto \omega^{-2\nu}$ with the exponent $2\nu \approx 1$ (see Fig. 3a), which is typical of intermittency phenomena [10].

The running-I state corresponds to a steady state. For instance, at the force $f = 0.35$ it survives for mesoscopic times $t > 2.5 \times 10^4 \tau_0$. For $0.256 \leq f \leq 0.485$ this state becomes slightly asymmetric, e.g., the top layer still remains attached to the top substrate, while the bottom layer, from time-to-time, detaches from the bottom substrate and moves over it as well as over the middle film layer, as can be seen from Fig. 2c. Atomic trajectories of the first layer show that it splits into immobile islands (“2D traffic jams”) and mobile “rivers” (channels) which,

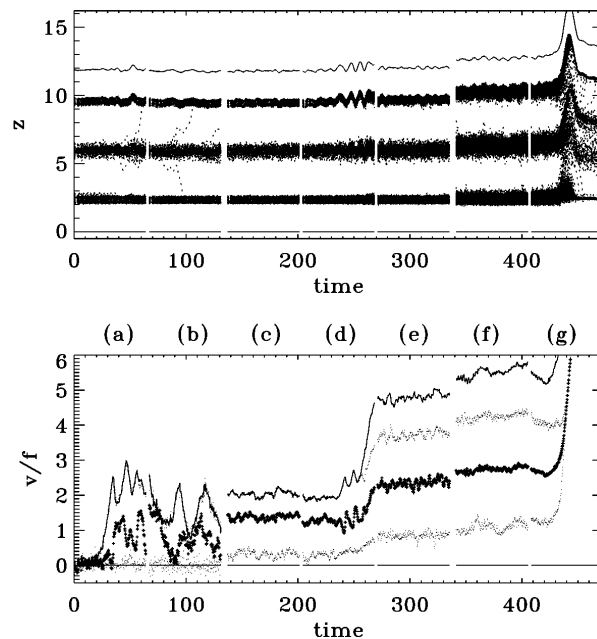


FIG. 2. System dynamics at different steady states [the curves (b), (c), (e), and (f)] and during transitions between them [(a), (d), and (g)]: (a) the transition from locked to running-I states, the force varies from $f_{\text{ini}} = 0.145$ to $f_{\text{fin}} = 2f_{\text{ini}}$ during the time $50\tau_0$; (b) $f = 0.146$, the steady state just after transition to the running-I state; (c) $f = 0.484$, the state before the transition to the running-II state; (d) the transition from running-I to running-II states, $f_{\text{ini}} = 0.485$ and $f_{\text{fin}} = 2f_{\text{ini}}$; (e) $f = 0.488$, the state after transition to the running-II state; (f) $f = 1.068$, the state before transition to the flying state; (g) the transition from running-II to flying states, $f_{\text{ini}} = 1.069$ and $f_{\text{fin}} = 2f_{\text{ini}}$. The top figure describes the z coordinates of the top and bottom substrates (the solid curves) as well as that of all atoms of the lubricant film (shown by dots). The bottom figure describes the x velocities of the substrates (the solid curves) and the velocities of the film atoms averaged over the layers: The middle layer is shown by plus signs, and the bottom and top layers by dots.

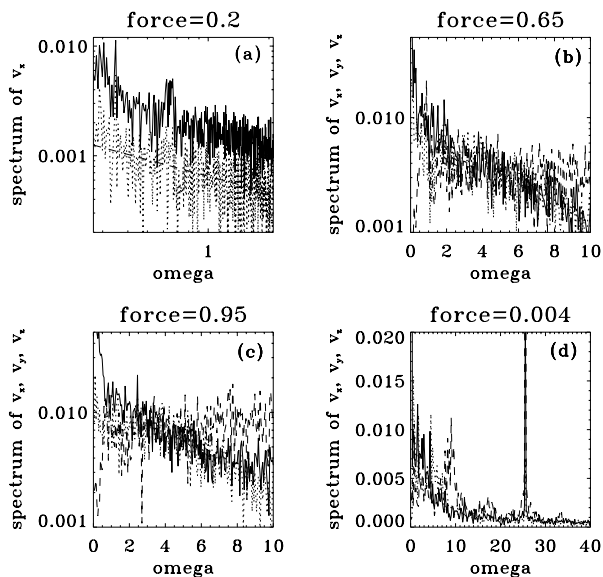


FIG. 3. Fourier spectra of atomic velocities: (a) for the running-I steady state. The solid curve corresponds to the x velocity averaged over all atoms of the lubricant, and the dotted curve to that averaged over the middle-layer atoms only. The dashed line describes the fit $A\omega^{-\nu}$ with $A = 0.65 \times 10^{-3}$ and $\nu = 0.5$; (b) and (c) for the running-II state; (d) for the flying state. In (b)–(d) the solid curves describe the x velocities averaged over all film atoms, the dotted curves correspond to the y velocities, and the dashed curves to the z velocities.

however, have an irregular shape contrary to what was observed for the 2D anisotropic FK model [6], where the rivers had a regular stripelike shape.

When f increases beyond the threshold $f'_s = 0.485$, the bottom and top layers detach from the corresponding substrates and begin to move with respect to them. During the transition to this “running-II” state, the average layer velocities are quite irregular (see Fig. 2d), and the trajectories show that, from time-to-time, immobile islands still emerge in the bottom and top layers.

(IIb) Additionally, for $0.256 \leq f \leq 0.485$, but in another simulation run, we also observed a different steady state, namely, the symmetric one (the curve labeled “a” in Fig. 1), where the first layer detaches from the bottom substrate and moves with velocity $\langle v_b \rangle \approx 0.25\langle v_s \rangle$, and similarly the top layer detaches from the top substrate.

(III) For $0.487 \leq f \leq 1.069$, the system is in the running-II state characterized by $\langle v_s \rangle \approx (4.5-5.5)f$ and $\langle v_b \rangle \approx (0.2-0.25)\langle v_s \rangle$ (see Figs. 2e and 2f). In this steady state all film layers are detached from the substrates, but there is a strong gradient of x velocities within the film in the z direction, i.e., the first layer slides over the bottom substrate, the middle layer slides over the first one, etc. The structure of the middle layer in the running-II state is almost perfectly the triangular solid-state symmetry. So this state corresponds to a “sliding solid” [5], or “running” state [6]. On the other hand, the structure of the bottom and top film layers is “solid” for $f < 0.8$, while at higher forces we observe the appearance of irregular (“chaotic”) stripes in these layers. One can see

that chaotic oscillations of the average velocity sharply increase for $f > 0.8$. For example, the spectrum of z oscillations in this regime seems to be pure white noise. Such a transition may be interpreted as the one from a laminar atomic flow to a turbulent motion inside a given (bottom or top) layer. With a further increase of force the chaotic oscillations increase, and at $f''_s = 1.07$ the intralayer laminar flow is destroyed and the system passes to the “flying” regime.

(IV) For $f \geq 1.07$ the lubricant film is detached from both substrates, and all film atoms move with approximately the same average velocity $\approx 0.5\langle v_s \rangle$. At the same time the lubricant is reorganized into a four-layer film (see Fig. 2g), so its width increases. The flying state is characterized by a very small effective friction $\eta_{\text{eff}} \equiv f/\langle v_s \rangle \sim 10^{-3}-10^{-4}$. When we turn off the force, the top substrate continues to fly with almost the same velocity owing to its inertia. To study the flying state for smaller v_s , we changed the simulation algorithm to a “constant-velocity” algorithm [2]. In this way we found that the flying state survives for forces as small as $f''_s \approx 0.001$. Taking a configuration obtained in the constant-velocity backward run, we then used it as the initial configuration for the constant-force run and checked that it was stable at such small forces. Figure 3d shows the Fourier spectrum for $f = 0.004$. In this case $\langle v_s \rangle \approx 23$, which corresponds to the “washboard” frequency $\omega_v = (2\pi/a_{sx})0.5\langle v_s \rangle \approx 24$. One can see that the peak at $\omega = \omega_v$ is well separated from the phonon spectrum of the lubricant; the latter has a cutoff at $\omega_{\text{max}} \approx 10$. Thus, there are no one-phonon channels for energy loss, so the effective friction is extremely low. Only when the washboard frequency reaches the value ω_{max} at $f \approx 0.001$ does the phonon damping channel open again, and the system returns to the locked state.

All of the steady-state regimes described above are separated by sharp (discontinuous) transitions, and if f decreases, the system exhibits hysteresis. Note also that, with an increase of the velocity of the top substrate, the distance between the substrates (the lubricant width) also increases from the value $z = 11.6$ at the beginning of the running-I state to the value $z = 12.7$ at the end of the running-II state. Then, just at the transition to the flying state, z jumps up (because of reorganization of the film from a three- to four-layer configuration) and finally stabilizes at the level $z = 13.3$ in the flying regime.

To more quantitatively characterize the running states, let us consider again the effective friction coefficient η_{eff} . Also, we introduce an effective friction coefficient η_m , which characterizes *intrinsic* energy losses of an atom of the middle layer when it moves, e.g., over the bottom film layer, and the friction coefficient η_b , which describes energy losses when an atom of the bottom layer moves over the bottom substrate. Then the total friction, acting on an atom of the bottom layer due to energy losses inside the layer and due to the external damping, is equal to $\eta + \eta_b$. When the bottom and middle layers move with

the velocities v_b and v_m correspondingly, we can write the balance of forces for the bottom layer as

$$(\eta + \eta_b)\langle v_b \rangle = \eta_m(\langle v_m \rangle - \langle v_b \rangle) + \eta(\langle v_s \rangle - \langle v_b \rangle), \quad (2)$$

and similar equations for the middle and top atomic layers. The equation for the force balance of the top substrate takes the form

$$N_s f = N_t \eta_b (\langle v_s \rangle - \langle v_t \rangle), \quad (3)$$

where $N_t \approx N_a/3 = 80$ is the number of atoms in the top film layer and v_t is its velocity. For the symmetric steady state we can take $\langle v_m \rangle = 0.5\langle v_s \rangle$ and $\langle v_t \rangle = \langle v_s \rangle - \langle v_b \rangle$, so Eqs. (2) and (3) yield $\eta_{\text{eff}}^{-1} = (2N_s/N_t)[\eta_b^{-1} + (\eta_m + 2\eta)^{-1}]$ and $\langle v_b \rangle/\langle v_m - v_b \rangle = (\eta_m + 2\eta)/\eta_b$. Now we can find the effective friction coefficients from the simulation data. For the case (IIa), taking $\langle v_s \rangle/f \approx 1.4-2$ from Fig. 1, we obtain $\eta_{\text{eff}} \approx 0.7 - 0.5$, $\eta_b = \infty$, and $\eta_m \approx 1.38 - 0.67$. For the case (IIb), taking $\langle v_b \rangle \approx 0.25\langle v_s \rangle$ and $\langle v_s \rangle/f \approx 3.5-4$, we obtain $\eta_{\text{eff}} \approx 0.29 - 0.25$, $\eta_b \approx 1.89 - 1.65$, and $\eta_m \approx 0.91 - 0.67$. Finally, for the running-II steady state, where $\langle v_b \rangle \approx (0.2-0.25)\langle v_s \rangle$, we have $\eta_{\text{eff}} \approx 0.22 - 0.18$, $\eta_b \approx 1.82 - 1.20$, and $\eta_m \approx 0.24 - 0.22$.

In conclusion, the incommensurate lubricant film we have modeled exhibits three different sliding regimes similar to those observed for the commensurate film [9]. The low-velocity regime corresponds to the stick-slip motion of the middle layer and is characterized by a relatively high effective friction. Energy losses in this regime are due to highly nonlinear dynamics of the system. In the intermediate-velocity regime the oscillatory component of the force applied to the film, due to alternating bond breaking and forming, with the washboard frequency ω_v , lies within the phonon spectrum of the layer. In this case the energy losses are due to one-phonon excitations in the lubricant, and the effective friction is relatively small. An estimation of η_m and η_b in this regime can be made by the method described in [11]. Finally, in the high-velocity regime, when the washboard frequency exceeds the maximum phonon frequency, the effective friction is very small.

Comparison with large scale MD simulations is hampered by the fact that our simulations are performed by slowly varying the driving force, and the closest MD simulations [4] used different loads and shear rate. Hence one might expect to access different types of states and obtain differing dependencies of sliding velocity on frictional force. However, different flow profiles, with or without slip at the substrate/film boundaries, have been observed, although as a function of applied load [4] or velocity [2] rather than as a function of driving force. Structural changes in the film, from fluid to solid, were observed in [4] as well as in our work, where we observed layers with solidlike structure in (III) and a "solid-with-defects" structure in (II).

Two other mechanisms of frictionless behavior have been predicted. First, when the film is in the truly incommensurate state (above the Aubry transition [12]), the static frictional force is zero, so one may expect that the kinetic friction will also be small. However, even small perturbations due to film motion could totally destroy such concerted motion, so there should be a special reason for this state to survive [13]. Second, when the sliding clusters have small sizes, their phonon spectra are discrete. Therefore, if the washboard frequency is smaller than the spacing of the phonon frequencies, phonon damping will not be operative [14]. On the other hand, the almost frictionless behavior predicted in the present work for the high-velocity regime, is much more robust and should be observed in many systems.

We gratefully acknowledge helpful discussions with M. Peyrard. This research is supported in part by the U.S. D.O.E. under Contract No. W-7405-ENG-36 and NATO Grant No. HTECH.LG.971372. O.B. was also partially supported by the Hong Kong Research Grant Council.

-
- [1] B. Brushan, J.N. Israelachvili, and Uzi Landman, *Nature* (London) **374**, 607 (1995); A. D. Berman, W. A. Ducker, and J. N. Israelachvili, *Langmuir* **12**, 4559 (1996); B. N. J. Persson, *Sliding Friction: Physical Principles and Applications* (Springer-Verlag, Berlin, 1998).
 - [2] J. E. Hammerberg *et al.*, *Physica* (Amsterdam) **123D**, 330 (1998); R. P. Mikulla *et al.* (to be published).
 - [3] J. Gao *et al.*, *J. Phys. Chem. B* **101**, 4013 (1997).
 - [4] P. A. Thompson, M. O. Robbins, and G. S. Grest, *Isr. J. Chem.* **35**, 93 (1995); A. Baljon and M. O. Robbins, *MRS Bull.* **22**, 22 (1997).
 - [5] B. N. J. Persson, *Phys. Rev. Lett.* **71**, 1212 (1993); *Phys. Rev. B* **48**, 18 140 (1993); *J. Chem. Phys.* **103**, 3849 (1995).
 - [6] O. M. Braun *et al.*, *Phys. Rev. Lett.* **78**, 1295 (1997); *Phys. Rev. E* **55**, 3598 (1997).
 - [7] O. M. Braun, A. R. Bishop, and J. Röder, *Phys. Rev. Lett.* **79**, 3692 (1997); O. M. Braun *et al.*, *Phys. Rev. E* **58**, 1311 (1998); M. Weiss and F.-J. Elmer, *Phys. Rev. B* **53**, 7539 (1996); *Z. Phys. B* **104**, 55 (1997).
 - [8] M. G. Rozman, M. Urbakh, and J. Klafter, *Europhys. Lett.* **39**, 183 (1997); *Phys. Rev. Lett.* **77**, 683 (1996); *Phys. Rev. E* **54**, 6485 (1996).
 - [9] O. M. Braun, T. Dauxois, and M. Peyrard, *Phys. Rev. B* **56**, 4987 (1997).
 - [10] H. G. Schuster, *Deterministic Chaos* (Physik-Verlag, Weinheim, 1984), Chap. IV.
 - [11] J. B. Sokoloff, *Phys. Rev. B* **42**, 760 (1990); **42**, 6745(E) (1990); B. N. J. Persson and A. Nitzan, *Surf. Sci.* **367**, 261 (1996); J. B. Sokoloff and M. S. Tomassone, *Phys. Rev. B* **57**, 4888 (1998).
 - [12] S. Aubry, *Physica* (Amsterdam) **7D**, 240 (1983).
 - [13] S. Aubry (private communication).
 - [14] J. B. Sokoloff, *Phys. Rev. Lett.* **71**, 3450 (1993); *Phys. Rev. B* **52**, 7205 (1995).